

# Materials Horizons

[rsc.li/materials-horizons](http://rsc.li/materials-horizons)



ISSN 2051-6347



COMMUNICATION  
S. Fujii *et al.*  
Pressure-sensitive adhesive powder

**175** YEARS



Cite this: *Mater. Horiz.*, 2016, 3, 47

Received 10th September 2015,  
Accepted 2nd October 2015

DOI: 10.1039/c5mh00203f

[www.rsc.li/materials-horizons](http://www.rsc.li/materials-horizons)

**Pressure-sensitive adhesive (PSA) powder consisting of particles with an adhesive polymer core and a hard nanoparticle shell morphology have been synthesized based on liquid marble technology. The PSA shows no adhesion in its original form, and shows its adhesive nature only after application of shear stress.**

## Introduction

Liquid marbles<sup>1–7</sup> are millimeter-sized liquid droplets stabilized by hydrophobic solid particles attached to the gas–liquid interface. Using liquid marble technology, it is possible to treat the liquid as a non-sticky powder. In nature, aphids, small sap-sucking insects, fabricate honeydew liquid marbles utilizing wax particles and treat the sticky liquid as non-wetting materials.<sup>8,9</sup> Recently, liquid marbles have attracted great attention in material science in view of their potential applications in transport & microfluidics,<sup>10–12</sup> cosmetics,<sup>13,14</sup> miniature reactors,<sup>15,16</sup> personal & health care products,<sup>17</sup> accelerometers,<sup>18</sup> sensors<sup>19–25</sup> and for gas storage.<sup>26,27</sup>

Pressure-sensitive adhesives (PSAs) are viscoelastic polymer materials that instantly adhere to solid surfaces *via* van der Waals forces (without covalent bonding) upon application of a light contact pressure.<sup>28,29</sup> PSAs are commonly applied in the form of a thin layer on a substrate or spraying droplets, and have found their applications ranging from simple tapes and labels to adhesives in automobile, aerospace and electronic industries.<sup>30–36</sup> Although the PSA tapes and spray droplets are useful materials, it is difficult to apply them to confined and intricate spaces due to their high viscosity.

<sup>a</sup> Department of Applied Chemistry, Faculty of Engineering, Osaka Institute of Technology, 5-16-1, Omiya, Asahi-ku, Osaka 535-8585, Japan.

E-mail: [syiji.fujii@oit.ac.jp](mailto:syiji.fujii@oit.ac.jp)

<sup>b</sup> Physics at Interfaces, Max-Planck Institute for Polymer Research, Ackermannweg 10, D-55128 Mainz, Germany

<sup>c</sup> Nanomaterials Microdevices Research Center, Osaka Institute of Technology, 5-16-1, Omiya, Asahi-ku, Osaka 535-8585, Japan

† Electronic supplementary information (ESI) available. See DOI: 10.1039/c5mh00203f

## Pressure-sensitive adhesive powder†

S. Fujii,<sup>\*a</sup> S. Sawada,<sup>a</sup> S. Nakayama,<sup>a</sup> M. Kappl,<sup>b</sup> K. Ueno,<sup>a</sup> K. Shitajima,<sup>a</sup> H.-J. Butt<sup>b</sup> and Y. Nakamura<sup>ac</sup>

### Conceptual insights

Pressure-sensitive adhesives (PSAs) are viscoelastic polymer materials that instantly adhere to solid surfaces *via* van der Waals forces upon application of a light contact pressure. PSAs are commonly applied in the form of a thin layer on a substrate or spraying droplets. Although the PSAs are useful functional materials, their sticky nature often makes them intractable, and there is a strong demand for development of easy handling PSAs. Here, we introduce a new concept for synthesizing PSA powder based on liquid marble technology. PSA powder consists of particles with a soft adhesive polymer core and a hard nanoparticle shell morphology, and shows no adhesion in its original form and flows like a powder. Only after application of shear stress, it then shows its adhesive nature. Adhesion is induced by rupture of the nanoparticle coating of the powder and outflow of the inner soft polymer. The PSA powder should be particularly useful in bonding in confined and intricate spaces, where sticky polymeric materials are difficult to apply due to their high viscosity.

Based on liquid marble technology, we describe a “PSA powder”, which consists of sticky PSA core covered by a shell of hard particles (Fig. 1). The key steps of the fabrication process are as follows: (1) synthesis of aqueous dispersion of soft polymer particles. This step controls tackiness. (2) Formation of liquid marbles by coating droplets of the latex dispersion with hydrophobic hard nanoparticles. (3) Evaporation of water from the liquid marbles. This process leads to soft adhesive polymer particles coated with hard nanoparticles, which show no adhesion and flow freely as powder. After applying shear stress, the material becomes adhesive, because the hard nanoparticle coating ruptures and the inner soft polymer is exposed. The PSA powder can be brought to confined and intricate spaces and can attain bonding by application of shear stress.

## Results and discussion

$\text{CaCO}_3$  nanoparticles were used as a liquid marble stabilizer, which were synthesized by the gas-slurry method in aqueous medium.<sup>37,38</sup> The number-average diameter was determined to



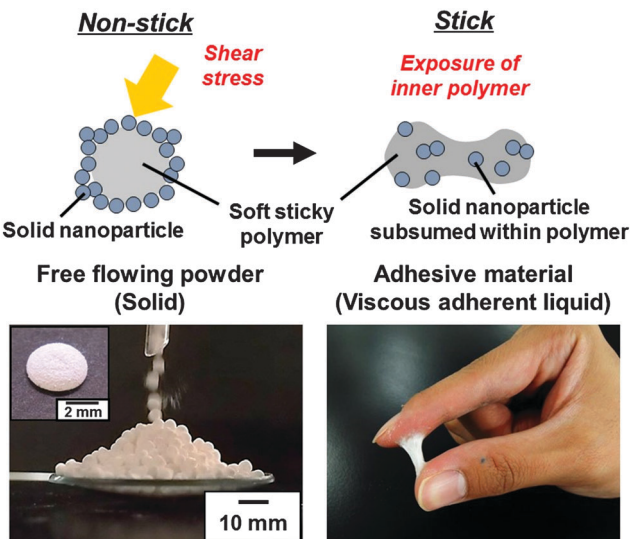


Fig. 1 Schematic representation of pressure-sensitive adhesive (PSA) powder consisting of particles with a soft sticky polymer core and a solid nanoparticle shell morphology. After application of shear stress, adhesive nature appeared because of outflow of the inner soft polymer. Optical photographs of such PSA materials are also shown. The PSA shows no adhesion in its original form and flows freely like a powder. (Inset shows single PSA particle.) Only after application of shear stress, it acts as an adhesive.

be 80 nm from transmission electron microscopy studies (Fig. S1, ESI<sup>†</sup>). The density was measured to be 2.52 g cm<sup>-3</sup> by a helium pycnometer. Octadecanoic acid was adsorbed to the nanoparticle surface *via* acid–base interaction between the carboxylic acid and CaCO<sub>3</sub> to render the CaCO<sub>3</sub> nanoparticles hydrophobic. The CaCO<sub>3</sub> nanoparticles existed as flocs with diameters between a few μm and 60 μm in air, which was confirmed by scanning electron microscopy (SEM) (Fig. S1, ESI<sup>†</sup>). The static contact angle of a water drop (15 μL) on hydrophobic CaCO<sub>3</sub> powder was measured to be 133 ± 3°.

Poly(*n*-butyl acrylate) (PBA) latex particles were synthesized by soap-free emulsion polymerization of *n*-butyl acrylate using ammonium persulfate free radical initiator in aqueous medium. PBA has glass transition temperature of ~54 °C.<sup>39</sup> It is popular as one of PSA base polymers, thanks to its optical clarity, stability against UV light and oxidation, and relatively low toxicity and cost. The hydrodynamic diameter of the PBA particles was measured to be 580 nm by dynamic light scattering. The zeta potential of PBA latex was -59 mV in distilled water (pH 6.5). The main causes for the anionic colloidal nature are persulfate anions used as initiators. Another cause for the negative potential is the spontaneous charging effects at the interfaces between the PBA particles and water as was discussed in a previous paper.<sup>40</sup> During the dialysis of PBA latex, the dispersion exhibited rather strong iridescent colors by the incident white light, which indicated that colloidally stable monodisperse PBA latex particles were successfully synthesized. The weight-average molecular weight and its distribution were determined to be 326 kDa and over 2.0, respectively, using gel permeation chromatography.

Individual 'liquid marbles' were prepared by rolling a 180 μL aqueous drop (solid content, 50.8 wt%) of PBA latex over dried

CaCO<sub>3</sub> powder.<sup>41</sup> The powder immediately coats the PBA latex drop and renders it both hydrophobic and non-wetting. These liquid marbles remained intact after transferring them onto a glass slide. They have significant surface roughness, which suggests that they are coated with CaCO<sub>3</sub> multilayers, rather than just a monolayer. The liquid marble shape was oblong and the volume decreased keeping the oblong shape on time scales of several hours at 25 °C due to water evaporation. After drying, CaCO<sub>3</sub> nanoparticle-coated PBA particles were obtained, which are also non-sticking to each other and to solid substrates (Fig. 1). This non-sticking behavior indicates that soft PBA component is covered with hard CaCO<sub>3</sub> nanoparticles and PBA does not contact with the substrate. SEM studies showed the existence of aggregates consisting of CaCO<sub>3</sub> nanoparticles on the surface of the particles even after removal of excess CaCO<sub>3</sub> powder (Fig. 2). The surface roughness of the liquid marble was estimated to be 26 ± 6 μm using a 3D laser scanning microscope (Fig. S2, ESI<sup>†</sup>). SEM studies of cryo-fractured particles confirmed that the liquid marble had the PBA-core/CaCO<sub>3</sub> nanoparticle shell morphology and that the PBA latex was film-formed (Fig. S3, ESI<sup>†</sup>). The weight ratio of PBA/CaCO<sub>3</sub> was gravimetrically calculated to be 98/2, assuming that the weight of CaCO<sub>3</sub> powder adsorbed to the 180 μL water drop is the same with that adsorbed to the 180 μL PBA aqueous latex droplet. Assuming that CaCO<sub>3</sub> nanoparticles were adsorbed to the surface of the PBA particle in close-packed manner, we estimate that, on average, the 'liquid marble' coating comprises 144 CaCO<sub>3</sub> particle overayers, which corresponds to an estimated

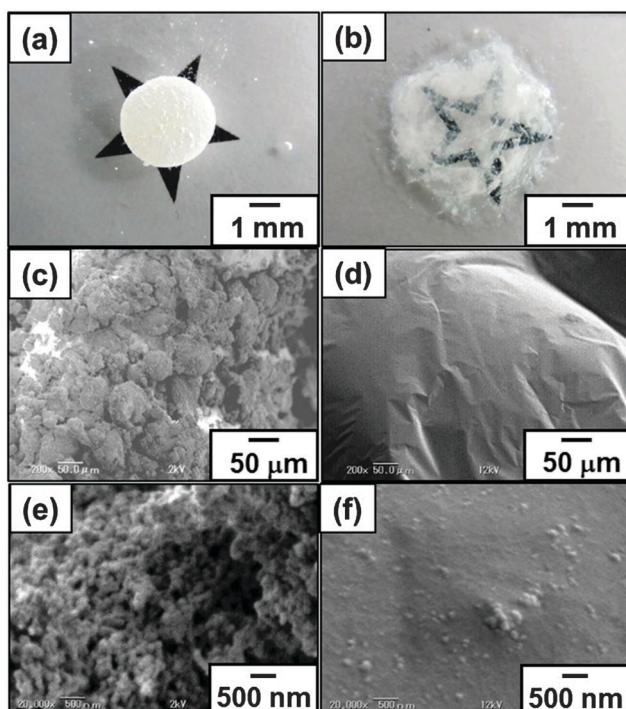


Fig. 2 (a and b) Digital photographs and (c–f) SEM images of a particle with a soft adhesive PBA core and a CaCO<sub>3</sub> hard nanoparticle shell morphology (a, c and e) before and (b, d and f) after application of shear stress.



thickness of 12  $\mu\text{m}$ . The calculated thickness was smaller than the surface roughness, which indicates the flocs of  $\text{CaCO}_3$  nanoparticles were adsorbed to the particle surface, as indicated by the SEM studies. Large-scale and continuous production of liquid marbles can be attained by spraying the latex droplets on the powder bed using an atomist spray.<sup>42</sup> This spray method is a rather facile and efficient approach for size control of liquid marbles: liquid marbles with wide range of sizes can be prepared by controlling nozzle diameter of the spray.

In order to study the transition of the dried PSA liquid marble from the non-sticky behavior to an adhesive material, we performed a series of compression/decompression tests. The dried liquid marble was placed on a metal plate and loaded from above by a metal piston with 10 mm diameter. After compressing the marble with a predefined load, the adhesion mediated by the dried adhesive liquid marble was measured during separation of the surfaces (Fig. 3a). By varying the applied load, we obtained typical adhesion *vs.* load curves as shown in Fig. 3b. For smaller loads (lower than approximately 11 N), we observed a monotonic and gradual increase in adhesion, which was related to the increase in contact area between  $\text{CaCO}_3$  overlayer on dried adhesive liquid marble and the metal surfaces due to plastic deformation of the PBA core. The applied load of approximately 11 N at the transition acting over a contact area of roughly 80  $\text{mm}^2$  corresponds to an average contact pressure of 0.14 MPa. When applying higher loads, there was a clear transition to a steeper and less regular increase of adhesion with load. This transition indicated the onset of tack due to contact of bare PBA exposed from the core with the metal surfaces. At these loads, the dried adhesive liquid marble was already flattened out sufficient to entirely cover the surfaces of the two metal plates and starting to bulge out over the edges of the metal plates. The exposure of bare PBA is most likely to occur first at the edge of the cylindrical piston, where stresses and shear should be maximized.

Probe tack test is a powerful method to investigate the adhesion properties for PSAs.<sup>43–48</sup> Compared to peel test, the probe tack test requires smaller amount of sample, it is possible to gain stress–displacement (S–D) tack curves, to control the contact time between adhesive polymer and probe precisely and to observe the debonding process using a camera.

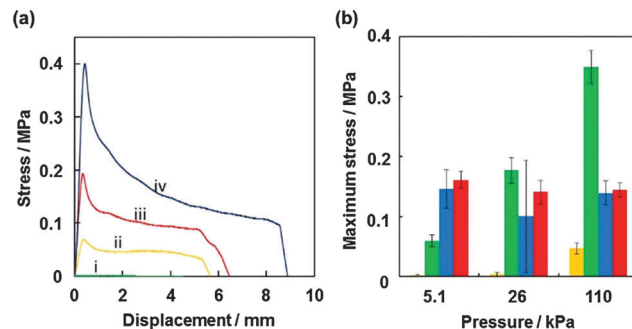


Fig. 4 (a) Stress–displacement tack curves obtained for PSA liquid marble: (i) before and (ii–iv) after application of shear stress. Pressure applied to PSA liquid marbles: (i and ii) 5.1, (iii) 26 and (iv) 110 kPa. (b) Relationship between pressure applied to PSA materials and maximum stress in tack measurement. Samples: liquid marble PSA (yellow bar) before and (green bar) after application of shear stress, (blue bar) PBA latex film with a thickness of 45  $\mu\text{m}$  and (red bar) commercially available PSA tape (Scotch<sup>®</sup> Magic<sup>™</sup> Tape 810).

For the probe tack measurement, smaller liquid marbles were prepared in order to prevent the PSA being squeezed out over the edge of the probe. The weight ratio of PBA/ $\text{CaCO}_3$  for the liquid marble prepared using 15  $\mu\text{L}$  PBA latex (50.8 wt%) was gravimetrically calculated to be 94/6. Fig. 4a shows representative S–D tack curves measured using the probe tack tester. The dried PSA liquid marbles before and after application of shear stress were placed on the stainless-steel probe: the PSA liquid marble was placed between release papers and kneaded using fingers for 30 s (40 reciprocating cycles). The glass substrate was reclined at 10  $\text{mm s}^{-1}$  and the sample on the probe brought into contact with the glass substrate. After a constant contact time (30 s), debonding started to occur when the glass substrate was elevated at 10  $\text{mm s}^{-1}$ . The S–D tack curve of the debonding process was recorded, and the maximum stress was determined from the curve. The pressures applied on the samples were controlled to be  $5.1 \times 10^3$  Pa ( $5.0 \times 10^2 \text{ kg m}^{-2}$ ),  $2.6 \times 10^4$  Pa ( $2.5 \times 10^3 \text{ kg m}^{-2}$ ) and  $1.1 \times 10^5$  Pa ( $1.1 \times 10^4 \text{ kg m}^{-2}$ ) by putting additional weights on the glass substrate. In the curve for the dried PSA liquid marble before application of shear stress, negligible stress ( $< 2.0 \times 10^{-3}$  MPa) was detected (curve i). The liquid marbles behave as non-sticky powder. The  $\text{CaCO}_3$  nanoparticles had negligible tack, and their presence at the liquid marble surface inhibits contact between the adhesive PBA and the glass and probe substrates. After kneading the liquid marble, stress reached a maximum point immediately after test initiation and then decreased gradually extending over a long range. The failure mode was a cohesive failure (curves ii–iv). Similar S–D curves have been observed for other PSA films.<sup>43–48</sup> SEM studies confirmed little presence of the  $\text{CaCO}_3$  nanoparticles on the surface of the kneaded PSA material, which indicates that PBA component was exposed at the surface and almost all the  $\text{CaCO}_3$  nanoparticles were subsumed within PBA matrix after application of shear stress, so the PBA component came into contact with the glass and probe substrates (Fig. 2). The surface roughness decreased from  $26 \pm 6 \mu\text{m}$  to  $4 \pm 1 \mu\text{m}$  after application of shear stress (Fig. S2, ESI<sup>†</sup>). Notably, the maximum

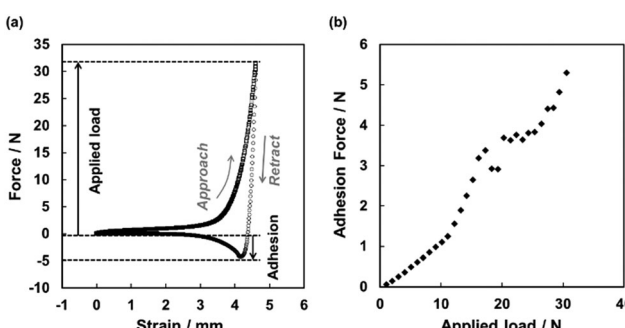


Fig. 3 (a) Example of force *vs.* strain curves obtained for PSA liquid marble, from which the dependence of adhesion on load was obtained: □, Approach; ○, Retract. (b) Dependence of adhesion on applied load.



stress increased to 0.40 MPa from  $4.7 \times 10^{-2}$  MPa upon application of higher pressure, due to an increase in contact area between the PBA and the substrate, which was confirmed using digital micrograph studies.

Maximum stress measured for dried PSA liquid marbles, PBA latex film and commercially available PSA tape (Scotch® Magic™ Tape 810) are shown in Fig. 4b, respectively. The PBA latex film showed lower maximum stress compared to those of liquid marbles. This should be due to the difference in contact area between PBA component and the substrates: the contact area between PBA latex film (45  $\mu\text{m}$  thickness) and the substrate was smaller than that between liquid marble (approximately 1 mm thickness) and substrate. Larger contact area could be attained thanks to thicker flowable PBA layer in the case of PSA powder after application of shear stress, but on the other hand full contact of PBA component with substrate cannot be attained in the case of PBA latex film because of thinner PBA film thickness and no complete parallel alignment of probe and substrate. Adhesion energy was defined as the energy dissipated during the debonding process and is proportional to the area under a tack curve. The adhesion energy also increased to 0.141  $\text{J m}^{-2}$  from 0.025  $\text{J m}^{-2}$  with an increase of applied pressure in liquid marble systems (Fig. S4, ESI†). The adhesion energies of the liquid marble systems were greater than those of the PBA latex film and PSA tape systems.

The optical properties of the PSA powder before and after application of shear stress have been assessed by visible absorption spectroscopy (ESI†). The transmittances measured at 600 nm for PSA powder before and after application of shear stress (thickness, 0.5 mm) were  $0.3 \pm 0.3\%$  and  $45 \pm 13\%$ , respectively. Whereas almost all of the visible light was scattered by the  $\text{CaCO}_3$  powder as an outer shell before application of shear stress, the  $\text{CaCO}_3$  nanoparticles were dispersed within PBA matrix and transparency increased significantly after application of shear stress.

## Experimental

### Materials

*n*-Butyl acrylate (BA; purity  $\geq 95.0\%$ ) was purchased from Sigma-Aldrich. Ammonium persulfate (APS; purity 95.0%) was purchased from Wako Chemicals.  $\text{CaCO}_3$  particles ( $D_h$ : 80 nm) were kindly donated from Shirashi Kogyo Kaisha; Ltd. Milli-Q water (Millipore Corp., MA, USA) with a specific resistance of  $18.2 \times 10^6 \Omega \text{ cm}$  was used in all experiments.

### PBA latex synthesis

PBA latex particles were synthesized as follows: APS (0.25 g) was added to water (250.0 g) in a 500 mL round-bottomed flask and the mixture stirred at 25 °C until APS was dissolved in water completely. The reaction mixture was then purged with nitrogen, and BA (25.0 g) was added. Soap-free emulsion polymerization was conducted at 65 °C for 24 h with magnetic stirring of 250 rpm. The resulting milky white colloidal PBA dispersion was purified using a dialysis membrane (Biotech CE Dialysis Tubing, MWCO: 100 kD, Spectrum Laboratories, Inc.) for two

weeks (distilled water in the dialysis container was replaced daily to remove impurities). After partial evaporation of water of the latex in dialysis membrane, solid content of the latex was tuned to be 50.8 wt% and then used as liquid phase of liquid marbles.

### Probe tack test

Tack of the adhesive samples was measured using a probe tack tester (TE-6002, Tester Sangyo, Saitama, Japan) with a stainless-steel (SUS 304) probe (5 mm diameter) at  $23 \pm 1$  °C (Fig. S5, ESI†). The dried adhesive liquid marbles before and after application of shear stress were placed on the stainless-steel probe: the dried adhesive liquid marble was put between release papers (Lintec Co., glassine type) and kneaded using fingers for 30 s (40 reciprocating cycles). The glass substrate (Micro Cover Glass, 18 × 18 No. 1, Matsunami Glass Ind., Ltd) attached to the substrate support (9.8 g) was set on the supporting board. The supporting board was reclined at 10  $\text{mm s}^{-1}$  and the sample on the probe brought into contact with the glass substrate. After a constant contact time (30 s), debonding started to occur when the supporting board was elevated at 10  $\text{mm s}^{-1}$ . Regarding the PBA latex film sample preparation, aqueous dispersions of the PBA particles were cast on 0.12–0.17 mm thick glass substrate, followed by heating at 70 °C for 24 h in an oven to evaporate the water. Then, the films were allowed to stand at 23–25 °C for one day. Thickness of the resulting PBA adhesive films was *ca.* 45  $\mu\text{m}$ , measured using a thickness gauge (Dial thickness gauge H-MT, Ozaki Mfg. Co. Ltd, Tokyo, Japan). The adhesive films placed on the glass substrate were attached to the film support (9.8 g), and the film support was set on the supporting board. The supporting board was reclined at 10  $\text{mm s}^{-1}$  and the probe brought into contact with the sample adhesive film. After a constant contact time (30 s), debonding started to occur when the supporting board was elevated at 10  $\text{mm s}^{-1}$ . The contact time of the tack specified by ASTM is 1 s.<sup>49</sup> We investigated tack properties of the PSA liquid marble with a contact time of 1 s, but unfortunately, it was difficult to obtain results with high reproducibility and the error bars for maximum stress and adhesion energy were large. This should be due to insufficient contact/wetting time of the PBA component to substrate. Results on the tack properties investigated at a contact time of 30 s were highly reproducible, and we used the data obtained. It is worth noting that there was no large difference in the tendency between the results with the contact times of 1 and 30 s, which has been also observed in our previous studies.<sup>50</sup>

The stress–displacement (S–D) curve of the debonding process was recorded, and the tack was defined as the maximum stress of the curve. The pressures applied on the samples were controlled to be  $5.1 \times 10^3$  Pa ( $5.0 \times 10^2 \text{ kg m}^{-2}$ ),  $2.6 \times 10^4$  Pa ( $2.5 \times 10^3 \text{ kg m}^{-2}$ ) and  $1.1 \times 10^5$  Pa ( $1.1 \times 10^4 \text{ kg m}^{-2}$ ) by putting additional weights on the glass substrate. The number of measurements was five and the data was shown with error bars. The top view of the adhesive liquid marbles contacting with the glass substrate was captured using a digital microscope (VW-6000, Keyence Corp., Osaka, Japan). The prism (20W × 20D × 20H mm)



was placed on the glass substrate, and the probe tip was observed through the prism from the front direction. The prism had a mass of 10 g and pressure was  $1.0 \times 10^3 \text{ kg m}^{-2}$ .

### Scanning electron microscopy

Scanning electron microscopy (SEM; Keyence VE-8800, 12 kV) was conducted with Au sputter-coated (Elionix SC-701 Quick Coater) dried samples.

### Digital photography

A digital camera (Ricoh Caplio R7;  $7.1 \times$  optical wide zoom lens) was used to record photographic images of the Janus colloidal crystal film.

### Material testing machine

A single dried adhesive liquid marble was placed on the stainless steel sample plate of a Zwick/Roell Z005 Universal Testing Machine with a load cell of 50 N. The marble was loaded from above with a cylindrical stainless steel piston with a diameter of 10 mm up to a predefined load at a speed of  $10 \text{ mm min}^{-1}$ . Upon reaching the predefined force, the movement of the piston was immediately reversed until full separation of the piston from the marble occurred. From the minimum in the retract curve, we obtained the adhesion force mediated by the marble. By increasing the applied load in steps of 1 nN, we obtained the dependence of the adhesion force on the applied load.

## Conclusions

In summary, we introduced a new concept for fabricating a PSA powder. The material can be prepared from liquid marbles containing an aqueous dispersion of soft polymer particles *via* evaporation of water. The PSA shows no adhesive character in its initial form and flows like a powder. After application of shear stress, the adhesive nature appeared induced by rupture of the  $\text{CaCO}_3$  nanoparticle coating and outflow of soft polymer. The PSA powder should be particularly useful in bonding in confined and intricate spaces (e.g. fastening screw and cracking of walls), where sticky polymeric materials are difficult to apply due to their high viscosity. Furthermore, the method for synthesis of nanoparticle-coated particles described here offers potential advantages: application of a wide range of polymers (vinyl and non-vinyl polymers), little energy to obtain dried products, easy incorporation of functional chemicals such as drugs, and easy conduction which needs no special apparatus. Using functional nanoparticles as a stabilizer will open up a new route to the preparation of a wide range of core-shell microspheres, which can be used in potential encapsulation/release applications.

## Acknowledgements

The authors wish to thank the following individuals: Prof. Shin-ichi Yusa and Mr Ryusuke Enomoto (Hyogo U) for their assistance in measuring hydrodynamic particle diameters and

zeta potentials, Ms Nozomi Karyu (Osaka Institute of Technology) for her assistance in tack measurements, Andreas Hanewald (MPI) for help with the material testing machine experiments, and Sumitomo Chemical for their assistance in measuring molecular weight of PBA. The authors also wish to thank reviewers for their valuable comments. This work was partially supported by JSPS-DAAD Bilateral Joint Research Projects and by a Grant-in-Aid for Scientific Research on Innovative Areas “Engineering Neo-Biomimetics,” “New Polymeric Materials Based on Element-Blocks” and “Molecular Soft Interface Science” from the Ministry of Education, Culture, Sports, Science, and Technology of Japan. Shiraishi Kogyo Kaisha; Ltd. Was thanked for kind donation of  $\text{CaCO}_3$  nanoparticles.

## Notes and references

- 1 P. Aussillous and D. Quéré, *Proc. R. Soc. A*, 2006, **462**, 973–999.
- 2 S. Fujii and R. Murakami, *KONA Powder Part. J.*, 2008, **26**, 153–166.
- 3 E. Bormashenko, *Curr. Opin. Colloid Interface Sci.*, 2011, **16**, 266–271.
- 4 G. McHale and M. I. Newton, *Soft Matter*, 2011, **7**, 5473–5481.
- 5 G. McHale and M. I. Newton, *Soft Matter*, 2015, **11**, 2530–2546.
- 6 L. Gao and T. J. McCarthy, *Langmuir*, 2007, **23**, 10445–10447.
- 7 D. Matsukuma, H. Watanabe, H. Yamaguchi and A. Takahara, *Langmuir*, 2011, **27**, 1269–1274.
- 8 N. Pike, D. Richard, W. Foster and L. Mahadevan, *Proc. R. Soc. B*, 2002, **269**, 1211–1215.
- 9 M. R. Weiss, *Annu. Rev. Entomol.*, 2006, **51**, 635–661.
- 10 M. I. Newton, D. L. Herbertson, S. J. Elliott, N. J. Shirtcliffe and G. McHale, *J. Phys. D: Appl. Phys.*, 2007, **40**, 20–24.
- 11 E. Bormashenko, R. Pogreb, Y. Bormashenko, A. Musin and T. Stein, *Langmuir*, 2008, **24**, 12119–12122.
- 12 J. R. Dorvee, M. J. Sailor and G. M. Miskelly, *Dalton Trans.*, 2008, 721–730.
- 13 C. Dampeiro, Cosmetic Laboratory Concepts-C.L.C, *WO Pat.*, 034917, 2005.
- 14 K. M. Lahanas, N. Vrabie, E. Santos and S. Miklean, *U.S. Pat.*, 6290941, Color Access, Inc., 2001.
- 15 Y. Xue, H. Wang, Y. Zhao, L. Dai, L. Feng, X. Wang and T. Lin, *Adv. Mater.*, 2010, **22**, 4814–4818.
- 16 T. Arbatan, A. Al-Aboodi, F. Sarvi, P. P. Y. Chan and W. Shen, *Adv. Healthcare Mater.*, 2012, **1**, 467–469.
- 17 T. Arbatan, L. Li, J. Tian and W. Shen, *Adv. Healthcare Mater.*, 2012, **1**, 80–83.
- 18 H. Zeng and Y. Zhao, *Appl. Phys. Lett.*, 2010, **96**, 114104.
- 19 E. Bormashenko and A. Musin, *Appl. Surf. Sci.*, 2009, **255**, 6429–6431.
- 20 D. Dupin, S. P. Armes and S. Fujii, *J. Am. Chem. Soc.*, 2009, **131**, 5386–5387.
- 21 J. Tian, T. Arbatan, X. Li and W. Shen, *Chem. Commun.*, 2010, **46**, 4734–4736.
- 22 V. Sivan, T. Shi-Yang, P. A. O’Mullane, P. Petersen, N. Eshtiaghi, K. Kalantar-zadeh and A. Mitchell, *Adv. Funct. Mater.*, 2013, **23**, 144–152.



- 23 K. Nakai, H. Nakagawa, K. Kuroda, S. Fujii, Y. Nakamura and S. Yusa, *Chem. Lett.*, 2013, **42**, 719–721.
- 24 K. Ueno, S. Hamasaki, E. J. Wanless, Y. Nakamura and S. Fujii, *Langmuir*, 2014, **30**, 3051–3059.
- 25 S. Yusa, M. Morihara, K. Nakai, S. Fujii, Y. Nakamura, A. Maruyama and N. Shimada, *Polym. J.*, 2014, **46**, 145–148.
- 26 W. Wang, C. L. Bray, D. J. Adams and A. I. Cooper, *J. Am. Chem. Soc.*, 2008, **130**, 11608–11609.
- 27 B. O. Carter, W. Wang, D. J. Adams and A. I. Cooper, *Langmuir*, 2010, **26**, 3186–3193.
- 28 D. Satas, *Handbook of Pressure Sensitive Adhesives*, 3rd edn, Van Nostrand Reinhold, New York, 1989.
- 29 A. Zosel, in *Advances in Pressure Sensitive Adhesive Technology*, ed. D. Satas, Satas & Associates, Warwick, RI, 1992, ch. 4, vol. 1.
- 30 J. L. Keddie, J. Mallégol and O. Dupont, *Mater. World*, 2001, **9**, 22–24.
- 31 L. Leger and C. Creton, *Philos. Trans. R. Soc.*, 2008, **366**, 1425–1442.
- 32 T. Wang, C.-H. Lei, A. B. Dalton, C. Creton, Y. Lin, Y.-P. Sun, K. A. S. Fernando, M. Manea, J. M. Asua and J. L. Keddie, *Adv. Mater.*, 2006, **18**, 2730–2734.
- 33 M. do Amaral, A. Roos, J. M. Asua and C. Creton, *J. Colloid Interface Sci.*, 2005, **281**, 325–338.
- 34 A. J. Crosby and K. R. Shull, *J. Polym. Sci., Polym. Phys.*, 1999, **37**, 3455–3472.
- 35 M. Toyama, T. Ito and H. Nukatsuka, *J. Appl. Polym. Sci.*, 1973, **17**, 3495–3502.
- 36 R. S. Gurney, D. Dupin, E. Siband, K. Ouzineb and J. L. Keddie, *ACS Appl. Mater. Interfaces*, 2013, **5**, 2137–2145.
- 37 S. Rigopoulos and A. Jones, *Ind. Eng. Chem. Res.*, 2003, **42**, 6567–6575.
- 38 S. Kakaraniya, A. Gupta and A. Mehra, *Ind. Eng. Chem. Res.*, 2007, **46**, 3170–3179.
- 39 J. Brandrup, E. H. Immergut and E. A. Grulke, *Polymer Handbook*, 4th edn, VI-199, Wiley, New York, 1999, vol. 1.
- 40 T. Okubo, *Colloids Surf.*, 1996, **109**, 77–88.
- 41 In control experiments, no liquid marbles could be formed under any conditions using bare  $\text{CaCO}_3$  powder without any surface treatment. These observations confirm the essential role played by the chemically-grafted hydrocarbon chains in promoting liquid marble formation.
- 42 S. Fujii, M. Suzuki, S. P. Armes, D. Dupin, S. Hamasaki, K. Aono and Y. Nakamura, *Langmuir*, 2011, **27**, 8067–8074.
- 43 C. Creton, J. Hooker and K. R. Shull, *Langmuir*, 2001, **17**, 4948–4954.
- 44 K. R. Brown and C. Creton, *Eur. Phys. J. E: Soft Matter Biol. Phys.*, 2002, **9**, 35–40.
- 45 T. Wang, C.-H. Lei, A. B. Dalton, C. Creton, Y. Lin, K. A. S. Fernando, Y.-P. Sun, M. Manea, J. M. Asua and J. L. Keddie, *Adv. Mater.*, 2006, **18**, 2730–2734.
- 46 T. Yamaguchi and M. Doi, *Eur. Phys. J. E: Soft Matter Biol. Phys.*, 2006, **21**, 331–339.
- 47 T. Wang, P. J. Colver, S. A. F. Bon and J. L. Keddie, *Soft Matter*, 2009, **5**, 3842–3849.
- 48 Y. Yamamoto, S. Fujii, K. Shitajima, K. Fujiwara, S. Hikasa and Y. Nakamura, *Polymer*, 2015, **70**, 77–87.
- 49 ASTM-D2979-71. Standard test method for pressure-sensitive tack of adhesives using an inverted probe machine, ASTM Standards Volume 15.06.
- 50 Y. Nakamura, K. Imamura, K. Yamamura, S. Fujii and Y. Urahama, *J. Adhes. Sci. Technol.*, 2013, **27**, 1951–1965.